# Supporting Information

**Experimental section**

*Synthesis of Ni-Co Prussian blue analogue (PBA) nanocubes:* The PBA cubes were synthesized according to the reference with little modification (*Adv. Mater.,* 2016, 28, 4601). In details, solution A was firstly prepared by dissolving 174.5 mg of nickel nitrate and 264.7 mg of sodium citrate in 20 mL of deionized water. Then solution B was prepared by dissolving 132.9 mg of potassium hexacyanocobaltate(III) in 20 mL of deionized water. Finally, solution B was added into solution A under magnetic stirring for 5 min, and the resultant mixed solution was aged for 24 h at room temperature.

*Synthesis of Ni-Co PBA nanocones:* 20 mg of the resultant PBA nanocubes were dispersed in 10 mL of ethanol under the assistance of ultrasonic. Then 20 mL of $H_2O$ containing 5 mL of concentrated $NH_3 \cdot H_2O$ (28%) was added into the above solutions, and stirred for 1 h at room temperature.

*Synthesis of Ni-Co mixed phosphide nanocones:* 10 mg of the resultant Ni-Co PBA nanocones and 100 mg of $Na_2H_2PO_2$ were placed at the two separate positions in one quartz tube with $Na_2H_2PO_2$ at the upstream side of the furnace, and then annealed at 350 $^oC$ for 2 h with a heating temperature rate of 2 $^oC\ min^{-1}$ in air. For comparison, the as-prepared Ni-Co PBA nanocubes were also annealed to prepare Ni-Co mixed phosphide hollow nanocubes under the same experimental conditions.

*Materials characterization*: X-ray diffraction (XRD) patterns were characterized on a Rigaku Miniflex 600 X-Ray Diffractometer (40 kV, 25 mA, Cu $K_\alpha$ radiation $\lambda$=1.5406) in the range of 20-80$^o$. The morphology and structure of the resultant products were investigated by scanning electron

microscopy (SEM, LEO FESEM 1530) equipped with energy-dispersive X-ray spectroscopy and transmission electron microscopy (TEM, JEOL, JEM-2100, 60 kV). The nitrogen adsorption-desorption isotherms of the resultant Ni-Co mixed phosphide and Ni-Co mixed phosphide hollow nanocubes were collected on a Quantachrome Instruments QuadraSorb SI4 system. Raman spectroscopy was recorded on a Bruker SENTERRA Raman system. Zeta potential was determined by Zetasizer Nano instrument (Malvern, Nano Z). X-ray photoelectron spectroscopy (XPS) spectra were recorded on an Axis Ultra (Kratos Analytical, UK) XPS spectrometer equipped with an Al Ka source (1486.6 eV).

*Electrochemical measurements*: The hydrogen evolution reaction performances of the resultant catalysts were carried out in a three-electrode system with a rotating glass carbon disk electrode (GCE) (PINE Research Instrumentation), graphite rod, and saturated calomel electrode (SCE) as working electrode, counter electrode, and reference electrode, respectively. The catalyst ink was prepared as following: 5 mg of catalyst was dispersed into 1 mL of ethanol containing 10 μL Nafion soloution (5wt%) under the assistance of sonication for 30 min. Then 20 μL of the catalyst ink was dropped onto the surface of GCE with the loading amount of 0.5 mg $cm^{-2}$ and dried under ambient conditions. Polarization curves were collected in 1.0 M NaOH and 0.5 M $H_2SO_4$ at a scan rate of 5 mV $s^{-1}$ with the speed rate of 1600 rpm. The stability tests were evaluated by cyclic voltammetry (CV) with a scan rate of 100 mV $s^{-1}$ from 0.05 V to -0.257 V vs. RHE in 1.0 M KOH and from 0.05 V to -0.233 V vs. RHE in 0.5 M $H_2SO_4$, respectively. All potentials were relative to reversible hydrogen electrode (RHE) by converting the measured potential vs. SCE according to the following equation: $E_{RHE} = E_{SCE} + 0.242 + 0.059 \times pH$. The overpotential (η) was calculated according to the following formula: $\eta = -E_{RHE}$. Electrochemical impedance spectroscopy (EIS) was performed to

determine the interfacial charge-transfer resistances for different modified electrodes in the frequency range from 0.1 Hz to 100 KHz with a perturbation signal of 5 mV. CV curves with different scan rate (10, 20, 30, 40, 50 mV $s^{-1}$) were measured in the potential range without redox processes to calculate the electrochemical double-layer capacitance as follows: $C_{dl} = I_c/\nu$, where $C_{dl}$, $I_c$, and ν are the double-layer capacitance (F $cm^{-2}$) of the electroactive materials, charging current (mA $cm^{-2}$), and scan rate (mV $s^{-1}$).

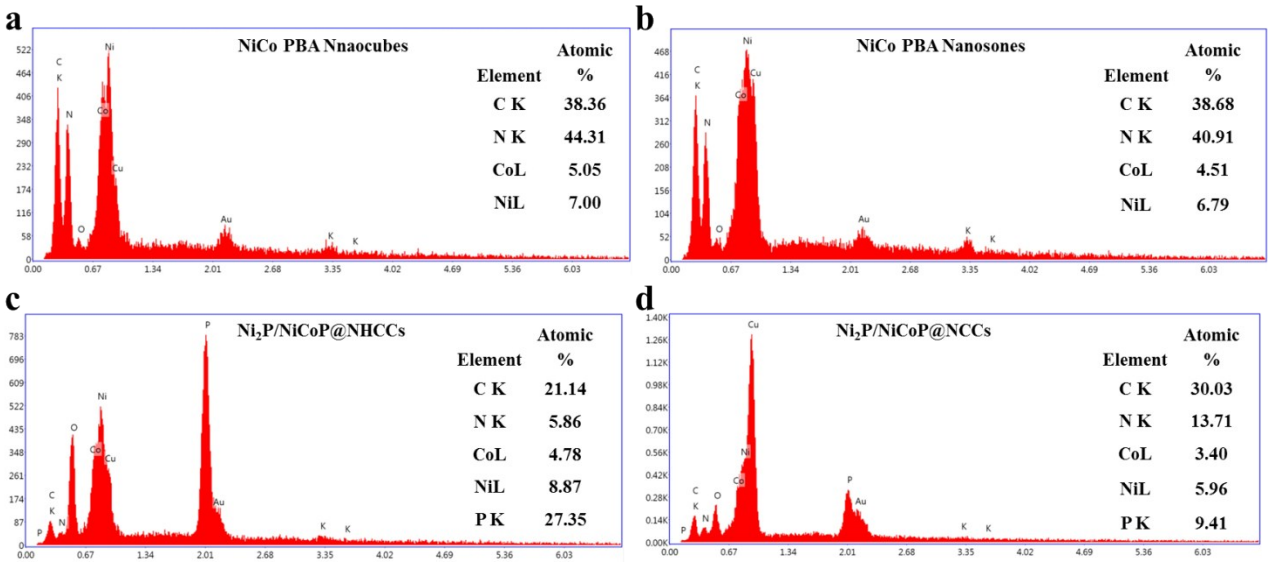


**Figure S1**. Energy Dispersive X-Ray Analysis (EDX) of (a) NiCo PBA nanocubes, (b) NiCo PBA nanocones by ammonia etching of NiCo PBA nanocubes, (c) $Ni_2P$/NiCoP@NHCCs byphosphide treatment of NiCo PBA nanocones and nanocubes and (d) $Ni_2P$/NiCoP@NCCs.

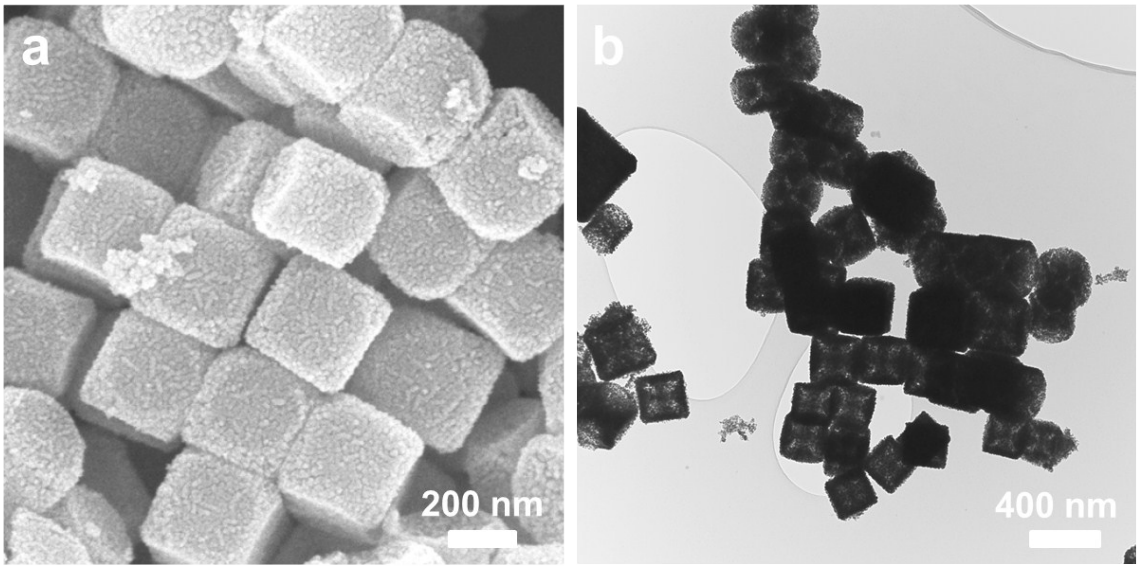


**Figure S2**. (a) SEM and (b) TEM images of NiCo PBA $Ni_2P$/NiCoP@N-doped hollow carbon nanocubes (NHCCs) by directly phosphide of NiCo PBA nanocubes.

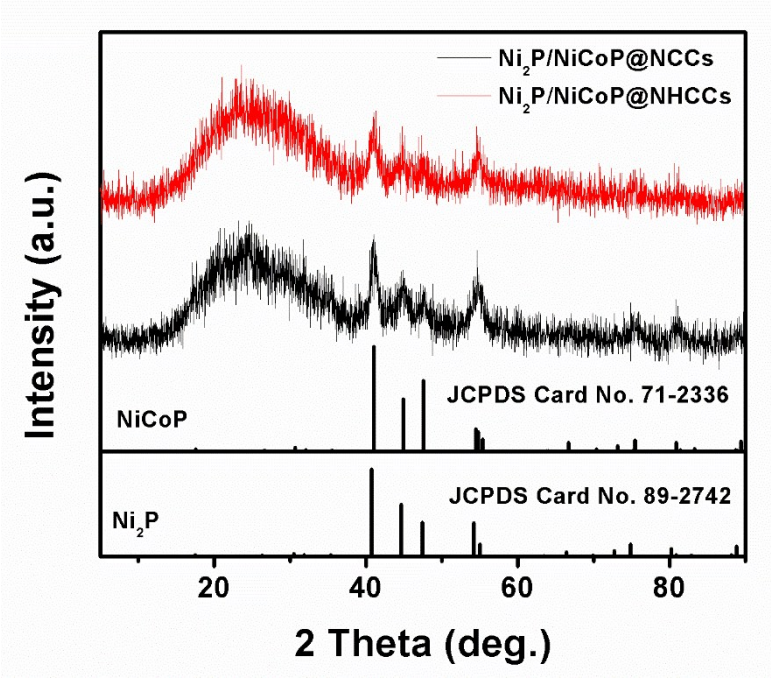


**Figure S3**. Powder XRD patterns of $Ni_2P$/NiCoP@NCCs and $Ni_2P$/NiCoP@NHCCs by phosphide treatment of NiCo PBA nanoones and nanocubes.

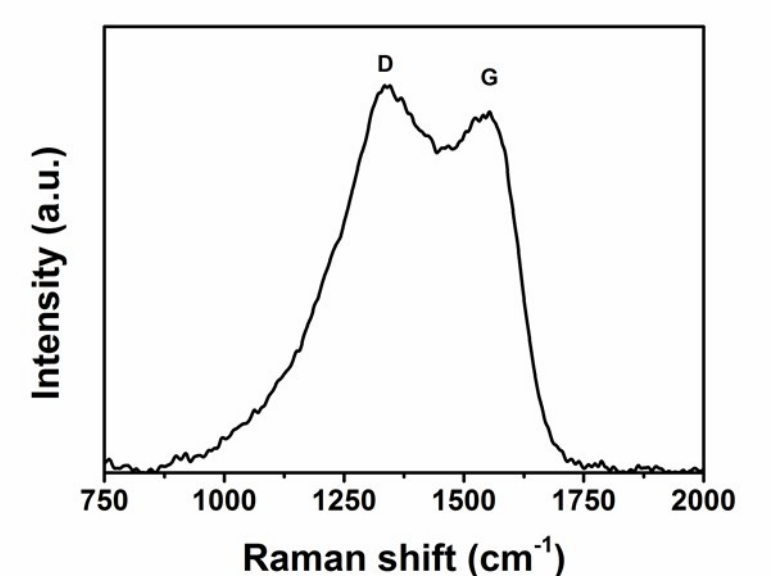


**Figure S4**. Raman spectra for $Ni_2P$/NiCoP@NCCs.

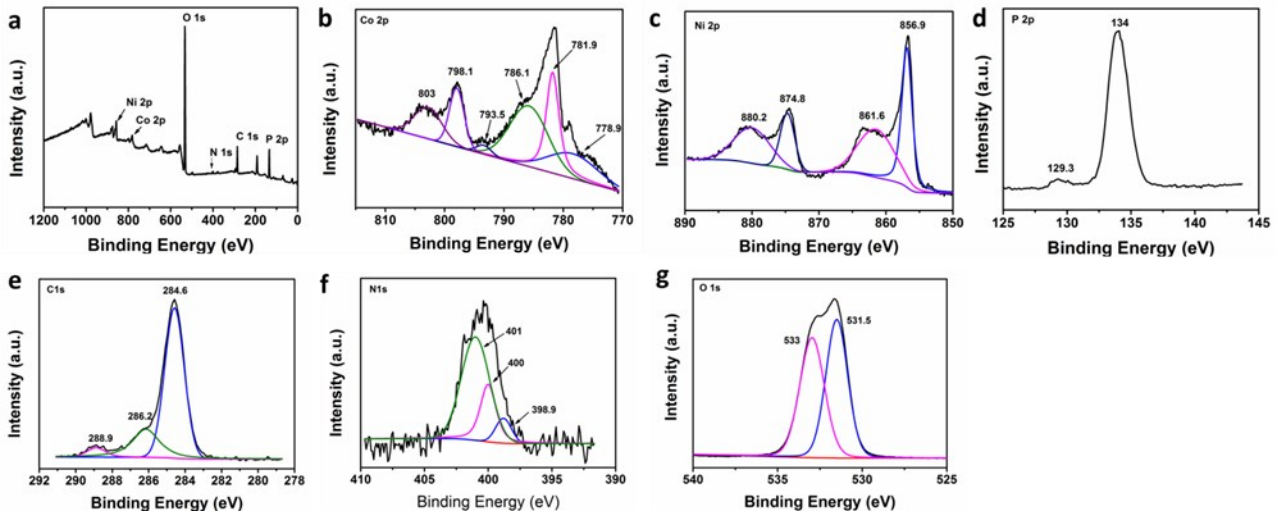


**Figure S5** XPS survey scans for $Ni_2P$/NiCoP@NCCs (a); High-resolution XPS spectra of (b) Co 2p, (c) Ni 2p, (d) P 2p, (e) C 1s, (f) N 1s, and (g) O 1s peaks for $Ni_2P$/NiCoP@NCCs.

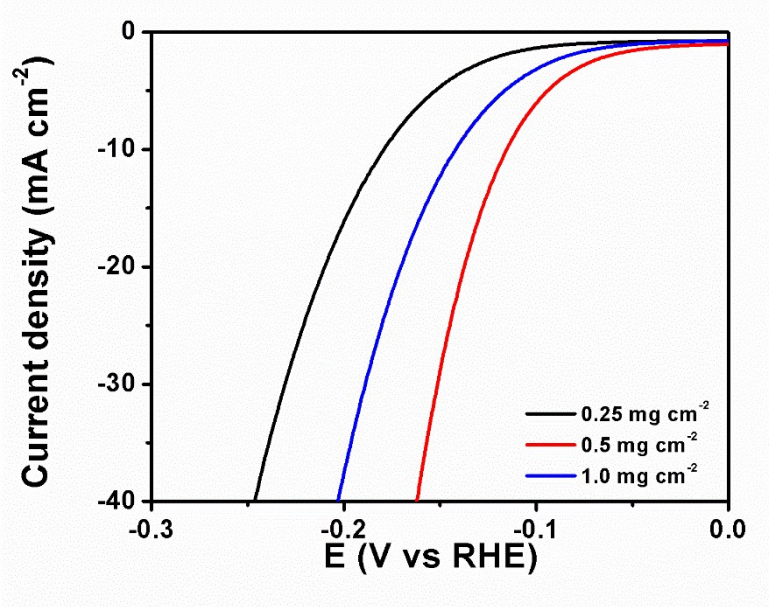


**Figure S6**. Polarization curves of the resultant $Ni_2P$/NiCoP@NCCs in 1.0 M KOH with different loading amount.

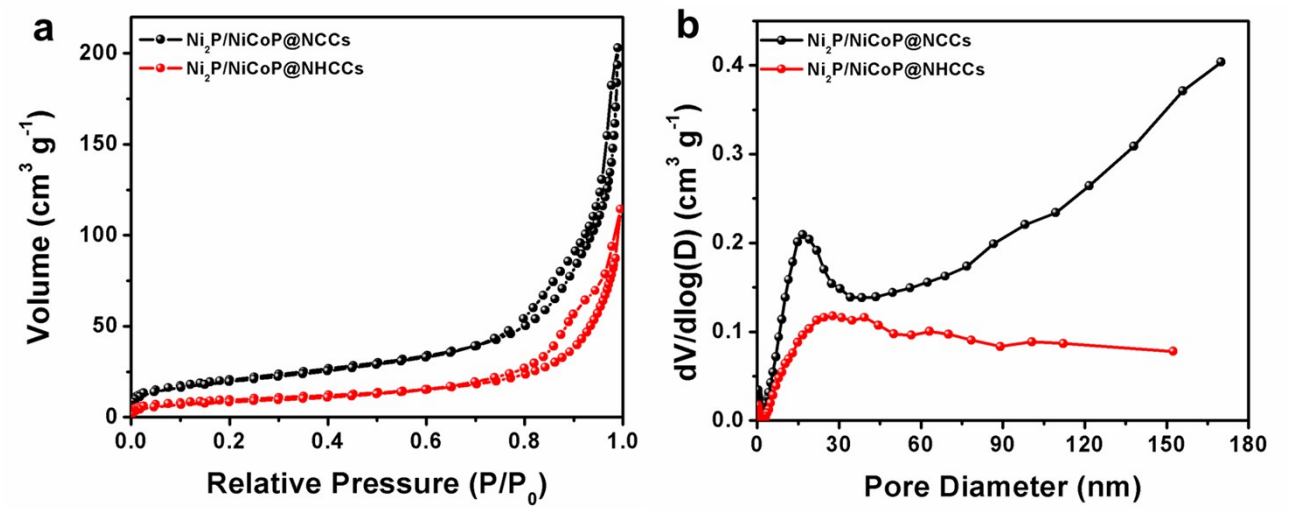


**Figure S7**. (a) Nitrogen adsorption–desorption isotherm and (b) Barret–Joyner–Halenda (BJH) pore size distribution plot of the as-prepared $Ni_2P$/NiCoP@NHCCs and $Ni_2P$/NiCoP@NCCs.

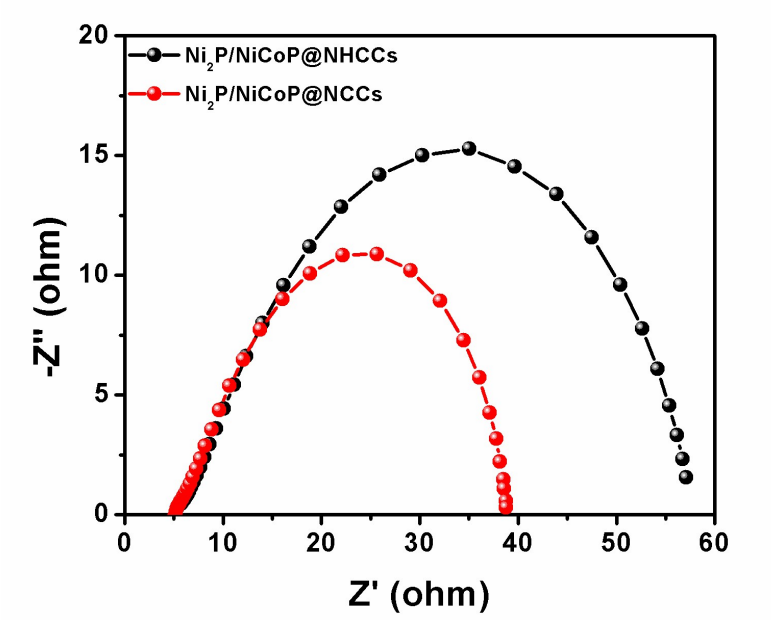


**Figure S8.** EIS plots of the as-prepared $Ni_2P$/NiCoP@NHCCs and $Ni_2P$/NiCoP@NCPs in 0.5 M $H_2SO_4$.

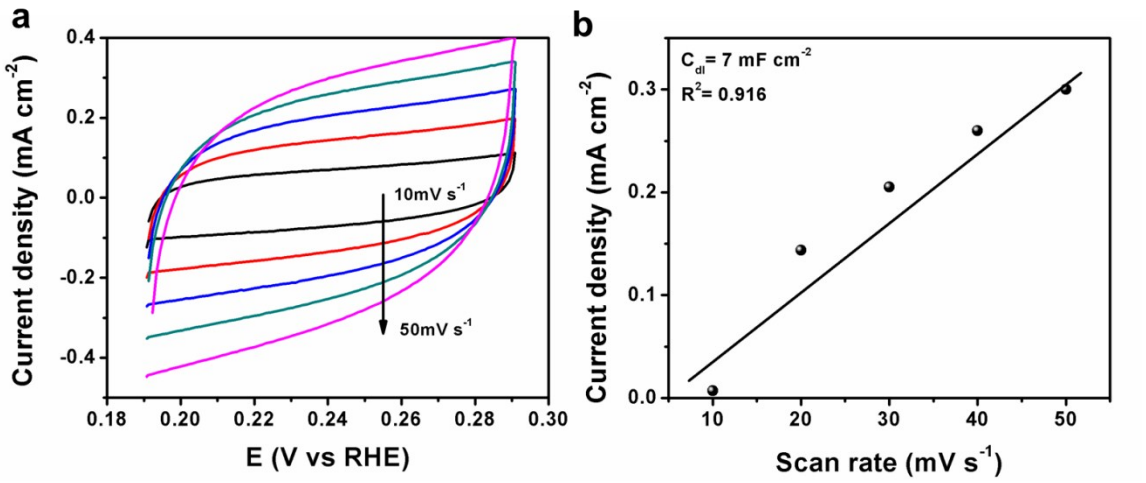


**Figure S9.** (a) Cyclic voltammogram (CV) curves of $Ni_2P$/NiCoP@NCCs in the double layer region at scan rates of 10, 20, 30, 40 and 50 mV $s^{-1}$ in 0.5 M $H_2SO_4$ aqueous electrolyte; (b) current density (taken at the potential of 0.24 V vs RHE) as a function of scan rate derived from (a).

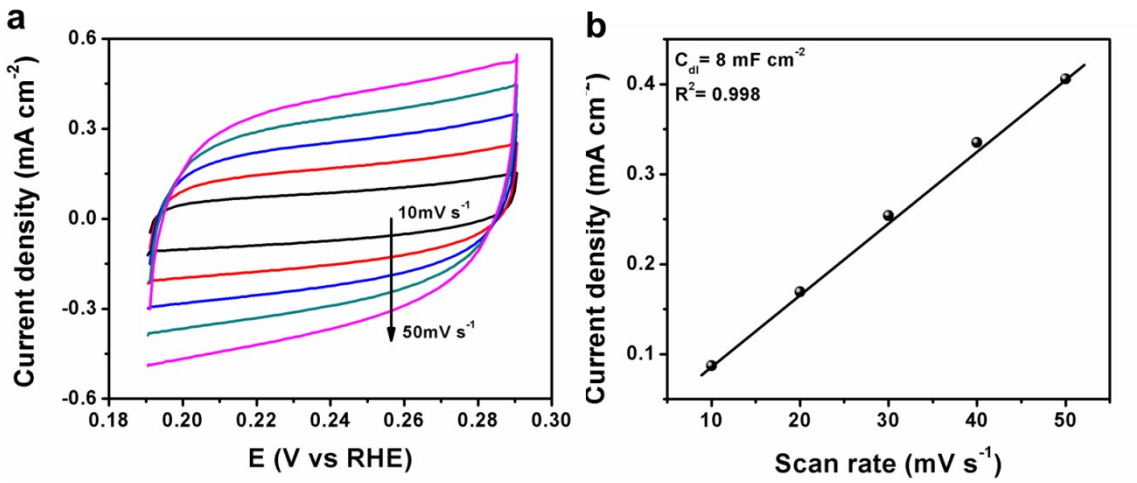


**Figure S10.** (a) Cyclic voltammogram (CV) curves of $Ni_2P$/NiCoP@NHCCs in the double layer region at scan rates of 10, 20, 30, 40 and 50 mV $s^{-1}$ in 0.5 M $H_2SO_4$ aqueous electrolyte; (b) current density (taken at the potential of 0.24 V vs. RHE) as a function of scan rate derived from (a).

**Table S1** Comparison of catalytic parameters of different HER catalysts.

| catalyst | electrolyte | Onset overpotential (mV vs RHE) | Overpotential at 10 mA $cm^{-2}$ (mV vs RHE) | Tafel slope (mV $dec^{-1}$) | Ref. |
|---|---|---|---|---|---|
| Porous CoP concave polyhedron | 0.5 M $H_2SO_4$ | 30 | 133 | 51 | [1] |
| CoP Hollow Polyhedron | 0.5 M $H_2SO_4$ | 35 | 159 | 59 | [2] |
| CoP/carbon nanotubes | 0.5 M $H_2SO_4$ | 64 | 139 | 52 | [3] |
| Porous $Ni_2P$ Polyhedrons | 0.5 M $H_2SO_4$ | 29 | 158 | 73 | [4] |
| 3D CoP/ graphene aerogels | 0.5 M $H_2SO_4$ | - | 121 | 50 | [5] |
| NiCoP quasi-hollow nanocubes | 1.0 M KOH | 133 | 150 | 60.6 | [6] |
| NiCoP Hollow Quasi-Polyhedra | 1.0 M KOH | 74 | 124 | 42 | [7] |
| CuCoP/nitrogen-doped carbon | 1.0 M KOH | - | 220 | 122 | [8] |
| Ni-Co mixed phosphide/nitrogen-doped carbon | 1.0 M KOH | 44.4 | 116 | 79 | This work |
| | 0.5 M $H_2SO_4$ | 51 | 120 | 79 | |

**Reference:**


[1] M. Xu, L. Han, Y. Han, Y. Yu, J. Zhai, S. Dong, *J. Mater. Chem. A* **2015**, *3*, 21471.

[2] M. Liu, J. Li, *ACS Appl. Mater. Interfaces* **2016**, *8*, 2158.

[3] C. Wu, Y. Yang, D. Dong, Y. Zhang, J. Li, *Small* **2017**, *13*, 1602873.

[4] L. Yan, P. Dai, Y. Wang, X. Gu, L. Li, L. Cao, X. Zhao, *ACS Appl. Mater. Interfaces* **2017**, *9*, 11642.

[5] X. Zhang, Y. Han, L. Huang, S. Dong, *ChemSusChem* **2016**, *9*, 3049.

[6] Y. Feng, X. Y. Yu, U. Paik, *Chem. Commun.* **2016**, *52*, 1633.

[7] Y. Li, J. Liu, C. Chen, X. Zhang, J. Chen, *ACS Appl. Mater. Interfaces* **2017**, *9*, 5982.

[8] J. Song, C. Zhu, B. Z. Xu, S. Fu, M. H. Engelhard, R. Ye, D. Du, S. P. Beckman, Y. Lin, *Adv. Energy Mater.* **2017**, *7*, 1601555.